

*XVII IMEKO World Congress  
Metrology in the 3rd Millennium  
June 22–27, 2003, Dubrovnik, Croatia*

## THE NEW IMPACT FORCE MACHINE AT PTB

*Michael Kobusch, Thomas Bruns*

Physikalisch-Technische Bundesanstalt (PTB), Braunschweig, Germany

**Abstract** – The prototype of a new facility for impulse force calibrations is presented in this paper. Furthermore, first experiences and measurements are described. Impulse forces are generated by a collinear impact of two cube-shaped bodies guided by linear air bearings. Traceability of force is realised by the determination of mass and acceleration, where the latter is derived from the velocity signal of a Laser-Doppler interferometer (LDI).

Keywords: impact, impulse force calibration, Laser-Doppler interferometry, air bearing.

### 1. INTRODUCTION

In recent years, the demand for precise impulse force measurements has increased due to the rising number of dynamic applications and due to improved safety standards, e.g. in the automotive industry. As the commonly performed static calibration of force transducers may lead to inexact results for dynamic forces, high precision demands a calibration method which works with dynamic forces of appropriate signal shape [1]. To cope with this problem, a new facility for impulse forces up to 20 kN has been developed and manufactured at PTB. This machine will assure high precision in the field of impulse force calibration for the first time.

The basic setup of the device is depicted in Fig. 1. It utilises two colliding masses with a force transducer mounted between them. Two cube-shaped stainless steel bodies of approximately 10 kg mass are guided by individual linear air bearings [2] in order to minimise friction. Moreover, in contrast to a pendulum impact force excitation [3], the collinear impact geometry guarantees a well-defined impact force vector orientation. This is especially important for the investigation of multi-component transducers.

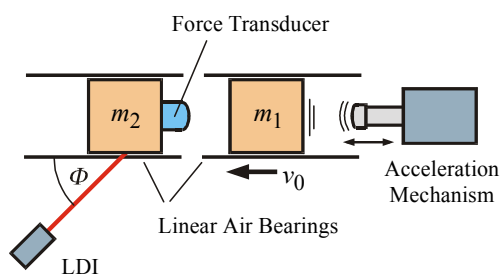


Fig. 1. Basic setup of the impact force machine

The cube (mass  $m_1$ ) on the right of Fig 1 is accelerated by a spring-driven mechanism to impact velocity  $v_0$  and impacts on the transducer under test mounted on the cube (mass  $m_2$ ) initially at rest. Using a Laser-Doppler interferometer (LDI) aimed at the cube's lateral side under oblique incidence (angle  $\Phi$ ), the corresponding line-of-sight velocity component  $v(t) \cdot \cos \Phi$  is measured. To assure a good signal quality of the retro-reflected measuring laser beam, a retro-reflector is applied to the surface [2]. The LDI velocity data is recorded with high sampling rate and analysed later. From the derived acceleration  $a(t)$  the inertial force  $F(t)$  is calculated according to Newton's law to be

$$F(t) = m a(t), \tag{1}$$

where  $m$  denotes the corresponding mass involved. This equation holds exactly for a rigid body, but it can give a good estimation for real bodies with elastic properties as simulations show [2]. In this regard it is remarkable that LDI can be easily applied to different surface points of interest whose acceleration data may be used for corrective measures.

### 2. TECHNICAL REALISATION

A photograph of the new facility for impulse force measurements at PTB is shown in Fig. 2.

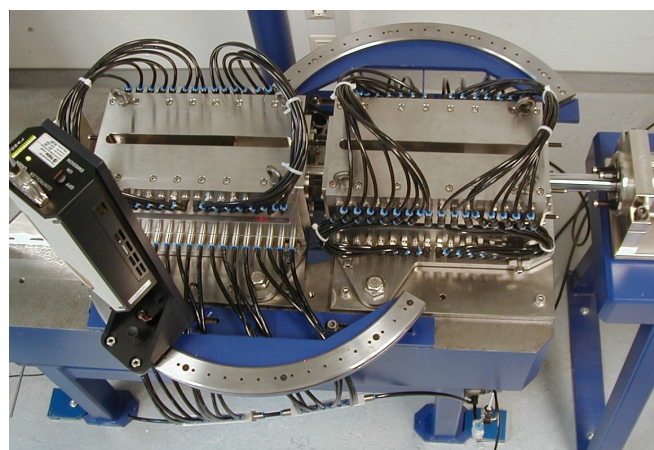


Fig. 2. Impact force machine

Two collinearly aligned linear air bearings are attached to a heavy iron cast plate of about 900 kg mass. This plate is decoupled from its basement via pneumatic springs. Mounted upside down, an LDI head (Polytec OFV 353) is

fixed to a holder which can be locked at 5° spacing on a bow-shaped rail. The vertically emitted LDI laser beam is deflected by a small mirror to the surface under examination which is accessed through a slotted hole in the air bearing plate. In addition, the rail can be axially shifted to measure at different points or to adapt to force transducers of different size. Shock absorbers mounted at the ends of the air bearings are used to slow down the moving bodies.

The spring-driven acceleration mechanism for the impacting mass is shown in Fig. 3. It is mounted onto a separate base in order to suppress pre-impact vibrations which would otherwise compromise the quality of the LDI measurement. Here, a strong compression spring drives a ram which accelerates the impacting mass. The spring is preloaded by a pneumatic actor, the release of the ball lock pin coupling (see right inset) is triggered manually. Furthermore, shock absorbers are used to protect against erroneously firing. To achieve different impact velocities, the compression of the preloaded spring can be adjusted within the range of 10 mm to 75 mm, its pre-set value is indicated by a scale (see left inset).

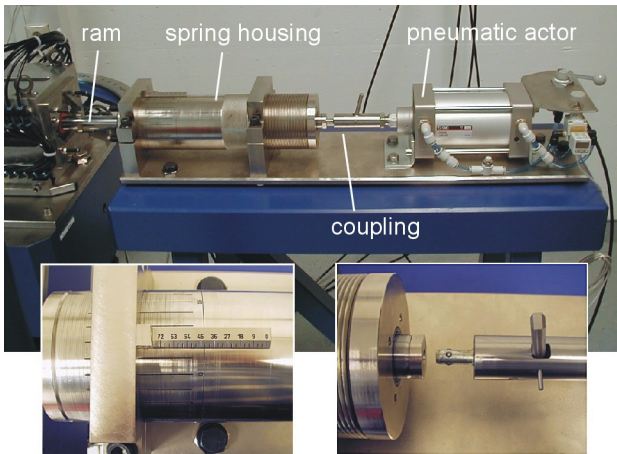


Fig. 3. Spring-driven acceleration mechanism

### 3. FIRST TESTS AND MEASUREMENTS

At present, the new device is going through an extensive test phase. System properties (e.g. uncertainties) have to be determined, flaws have to be uncovered and eliminated, and a lot of experience with impulse force measurements will be gathered.

#### 3.1. LDI beam angles

The Laser-Doppler interferometer measures the line-of-sight velocity component of the moving mass. Therefore, the precise knowledge of the applied beam angle  $\Phi$  is crucial for the accuracy of the force measurement. For example, to achieve 0,1 percent uncertainty of velocity measured at  $\Phi = 45^\circ$ , its uncertainty  $\Delta\Phi$  must be less than  $0,06^\circ$  [1].

To determine the beam angles obtained at different LDI holder positions, a second LDI was simultaneously directed at the front under perpendicular beam incidence (Fig. 4). Here, the shock absorber mounted at the left air bearing had to be removed beforehand. For measurements at the right bow-shaped rail, the left steel cube was removed too.

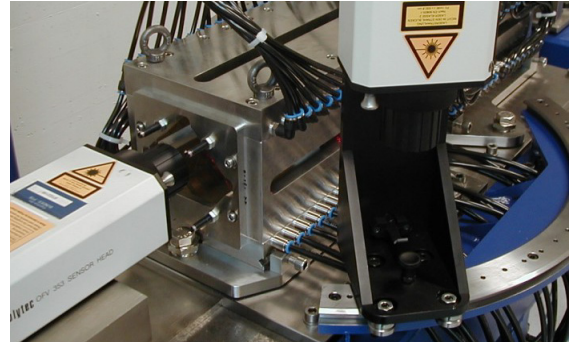


Fig. 4. Measurement of LDI beam angles

Using the LDI fringe counter outputs, the optical path length of the slowly gliding steel cubes was measured with sub-wavelength resolution. The comparison of both LDI values, length  $p$  measured at beam angle  $\Phi$  and reference length  $p_0$  at perpendicular incidence, respectively, leads to the expression

$$\Phi = \arccos(p / p_0) \quad (2)$$

The experimentally derived beam angles of the indexed LDI holder positions are displayed in Fig. 5 for both masses or bow rails, respectively. The diagram shows the respective deviation from the nominal beam angle. It is obvious that the deviation from the nominal values is up to  $0,3^\circ$  and that a high precision as mentioned is not achieved here through manufacturing and assembling. Therefore, the measurement of beam angles is absolutely necessary.

Furthermore, repetitive measurements (10 repetitions) at both masses and six positions each yield maximum standard deviations of less than  $0,002^\circ$  beam angle. In contrast, the reproducibility after re-positioning of the LDI holder is of the order of  $0,01^\circ$ , whereas after disassembling of the interferometer the angles may differ by as much as  $0,2^\circ$ .

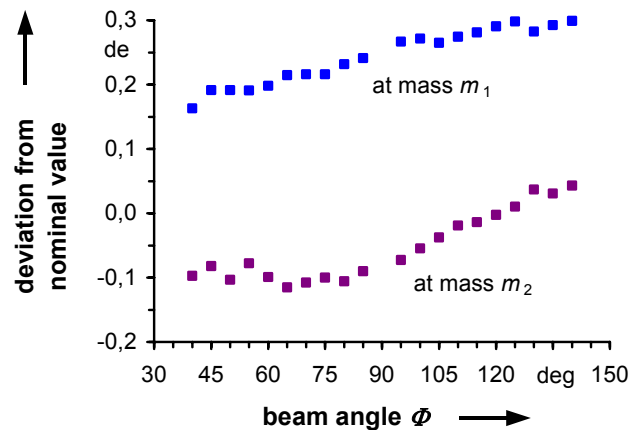


Fig. 5. Measured LDI beam angles

#### 3.2. Velocity Signal

First impact tests were performed with a sensor replica and a spherical loading pad of Teflon (total mass 123 g, overall dimensions  $\varnothing 30$  mm x 62 mm). As before [2, 3], strips of retro-reflective adhesive sheeting using high index glass spheres (diameter about  $60 \mu\text{m}$ ) were applied at the surfaces under observation. Due to the optically rough surface of unevenly distributed micro spheres of different

size (cf. Fig. 6), the retro-reflected beam of coherent light suffers from strong speckle noise which leads to a corresponding noisy velocity signal when the laser beam scans over such a surface.

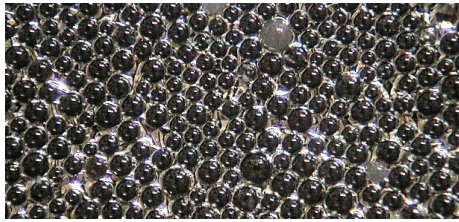


Fig. 6. Micro-photograph of the retro-reflective adhesive sheeting

To overcome this speckle noise, the optically rough surface has to be replaced by a smooth retro-reflective surface, e.g. like that of a triple prism or an adequately orientated mirror, respectively. When applying reflectors with conventional mirror surfaces the problems arising from the additional mass, its mechanical coupling, a small geometrical operating range and a lateral beam shift have to be taken into consideration. A different way to achieve a speckle-free reflection is the use of a diffraction grating, which retro-reflects a diffracted beam at certain angles [4]. Indeed, such a reflector can be directly applied at the surface under test, e.g. by photo lithography.

In order to test this kind of reflector, a radial strip cut from a CD-RW disc (groove spacing of about 1,5 μm) was applied to the trailing side of the moving mass cube (Fig. 7), while its leading side still bears the adhesive sheeting. The measurement shown in Fig. 8 compares the LDI signal quality obtained with both retro-reflectors during a 80 ms time span just before impact. For this example, the impact velocity  $v_0$  was 0,65 m/s, the beam angle 65°.

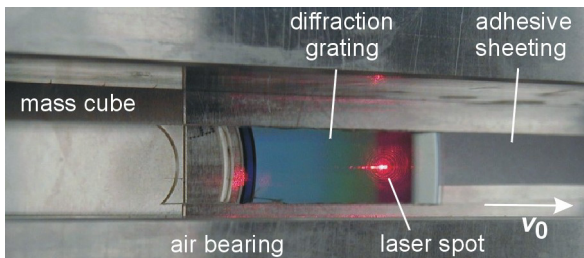


Fig. 7. Retro-reflectors attached to the lateral side of the mass cube

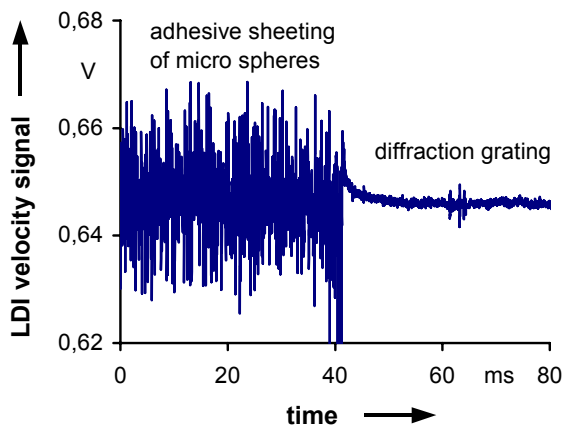


Fig. 8. Signal noise of the LDI velocity signal

Compared to the retro-reflective adhesive sheeting, the noise associated with the diffraction grating is 15 times smaller.

### 3.3. Acceleration mechanism

Figure 9 shows the experimentally derived characteristic of the spring-loaded acceleration mechanism. Here, the achieved impact velocity  $v_0$  of the accelerated 10 kg mass cube  $m_1$  is plotted against the pre-set spring compression  $x$ . At each of the 20 points, three repetitive measurements were made. The diagram demonstrates that the impact velocity is a linear function of the spring compression with the relation

$$v_0 = 0,03714 \text{ m/s} \cdot x / \text{mm} \quad (3)$$

obtained by a regression analysis. In the upper range, the deviation from linearity is less than about 0,4 %, whereas in the lower range, deviations of up to 4 percent may occur due to the increased relative influence of residual friction at smaller spring energies. In general, these results prove that the acceleration mechanism produces impact velocities of very satisfying reproducibility.

Moreover, the analysis of the LDI data shows that the impulse force duration is almost independent of impact velocity. Here, resulting from the elastic properties of the tested configuration of sensor replica and loading pad, the typical duration was 1,4 ms.

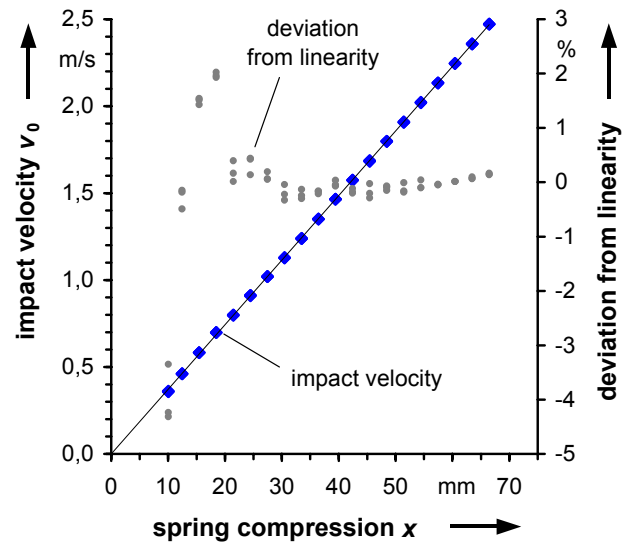


Fig. 9. Impact velocity vs. spring compression of the acceleration mechanism

### 3.4. Impulse force measurements

Figure 10 shows a photograph of the mounted piezo-electric force transducer of 20 kN capacity used for first impulse force measurements. The force was transmitted through the previously described elastic Teflon loading pad used again here.

The preliminary results yield that impact pulses measured by the piezo-electric force transducer are of very good reproducibility regarding pulse shape, pulse amplitude and even small superposed vibrational components. Compared to pulses obtained with the sensor replica, the pulse duration is almost the same.

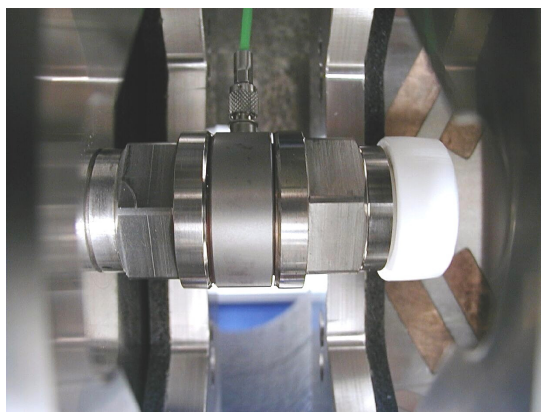


Fig. 10. Mounted piezo force transducer with loading pad

The following example (Fig. 11) shows a typical pulse of 1,3 ms duration and 7,5 kN peak amplitude recorded at a sample rate of 100 kSample/s. As expected from the reproducibility of the impact velocity, repetitive measurements were almost indistinguishable. In order to quantify the reproducibility of impulse force generation, the small scatter in impact velocity has to be compensated. Here, the impact velocities of  $m_1$  and the corresponding velocities of  $m_2$  after impact are assumed to be proportional, as the LDI measurement was only performed at  $m_2$ . Thus, by normalising the force signal to the maximum velocity after impact, the derived peak amplitudes show a standard deviation of just 0,1 %. This result demonstrates that impact forces can be generated with very good precision.

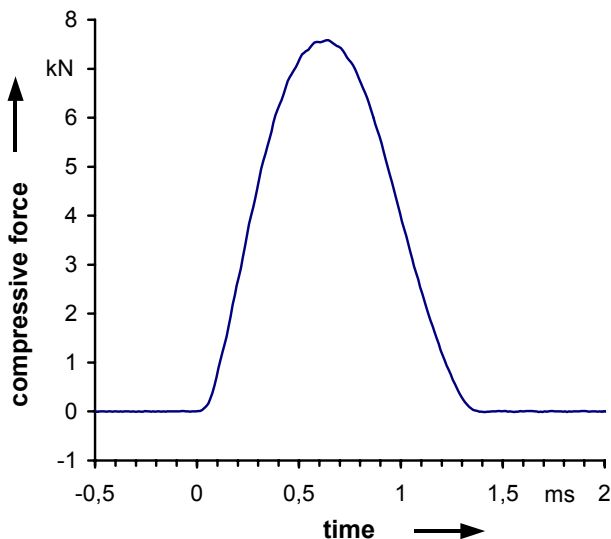


Fig. 11. Impact pulse measured by the piezo-electric transducer

At close inspection, the force pulse shows small ripples which can be well-analysed after appropriate high-pass filtering of the pulse data. The normalised signal filtered by a Butterworth high-pass of 4<sup>th</sup> order and 10 kHz corner frequency is displayed in Fig. 12. It is obvious that a damped oscillation of 15 kHz was excited at the onset of impact at time zero. This frequency agrees well with the theoretical vibrational mode of the transducer’s end mass [1], where a value of 17,3 kHz can be calculated from the specified sensor stiffness and the measured masses of the

transducer (50 % assumed) plus its attached loading pad. The filtered signal further demonstrates the good reproducibility of the measured pulses, since the vibrational signal component resulting from the time-averaged mean of five measurements cannot be distinguished from a single measurement.

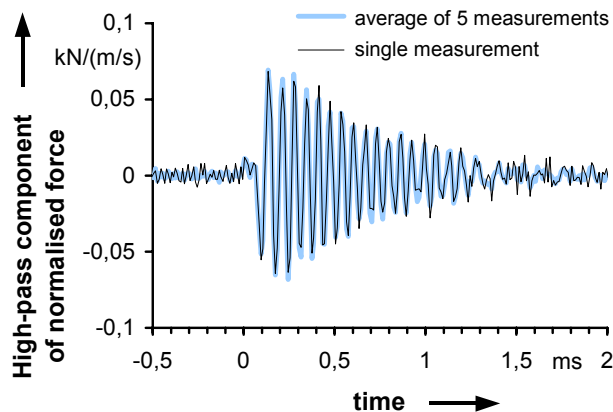


Fig. 12. High-pass filtered normalised force signal

A comparison of the signals measured by the piezo-electric force transducer and the traced forces based on LDI-measurements is shown in Fig. 13 for the inertial force at mass  $m_1$  and mass  $m_2$ , respectively. Due to the good reproducibility of impulse force generation, simultaneous LDI measurements at both masses were not necessary here. Thus, the figure presents different measurements (set of 3 time-averaged signal each) normalised to the peak force signal of the piezo-electric transducer which serves as the reference.

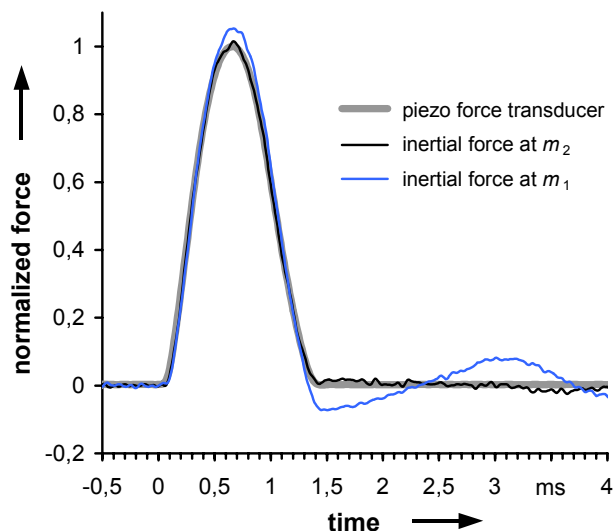


Fig. 13. Impact pulse measured by the piezo-electric transducer and the optically traced inertial forces at mass  $m_1$  and  $m_2$

For these preliminary measurements, traceability of force by LDI was accomplished by using a grating retro-reflector and a beam angle of 65°. The analogue signals of LDI (low-pass filtered with 20 kHz) and force transducer were sampled and recorded at 100 kHz. In order to suppress noise which is strongly amplified by the differentiation process

applied to the LDI velocity data, all signals were passed through a digital low-pass filter of 10 kHz corner frequency (Butterworth filter of 4<sup>th</sup> order).

It is clearly seen that the inertial peak force of the accelerated mass  $m_2$  agrees quite well with that of the piezo-electric force transducer. The deviation comes to about 1,5 %. In contrast, the measured inertial peak force of the impactor  $m_1$  has a deviation of about 5 %. But in theory, the latter value should be just one percent higher than the referenced piezo force due to the acting additive inertial force component of the transducer's end mass. Obviously, a more or less pronounced vibrational component of about 300 Hz was superposed in both LDI signals, which easily explains the measured deviations. Further experiments indicate that this disturbance results from a rotational vibration of the masses which was excited after impact. Causes for the excitation of that vibration could be the non-axial alignment of the air bearings and an off-axis contact point or an asymmetrical pressure distribution at the transducer's loading pad. In order to eliminate or reduce this problem, further investigations have to be made.

However, these first experiments indicate that the tested piezo-electric force transducer is well-suited for such applied pulse durations. Future experiments with different types of loading pads leading to force pulses of different duration and improvements of signal quality will give more precise information about the quality of this sensor regarding impact applications.

#### 4. CONCLUSIONS

The new impulse force calibration machine of PTB is presented in this paper. First experimental results show that the impact of the two collinear guided steel cubes generates impulses of very good reproducibility. In preliminary tests, a piezo-electric force transducer was investigated with force pulses of 1,3 ms duration. The comparison of force measured by the transducer and its optically traced force at the accelerated mass cube proves that this transducer is well-suited for measuring pulses of such duration.

In the near future, more experience will be gained which leads to a better understanding of the machine's properties, as well as that of suitable impulse force transducers. In addition, this prototype impulse force machine will be optimised and will open up new prospects for high precision impulse force measurements in future.

#### REFERENCES

- [1] Th. Bruns, R. Kumme, M. Kobusch, M. Peters, "From oscillation to impact: the design of a new force calibration device at PTB", *Measurement*, vol. 32, pp. 85-92, 2002.
- [2] Th. Bruns, M. Kobusch, "Impulse Force Calibration: Design and Simulation of a New Calibration Device", *Proceedings of the 17<sup>th</sup> International Conference on Force, Mass, Torque and Pressure Measurements, IMEKO TC3*, Istanbul, Turkey, pp. 85-91, 17-21 Sept. 2001.
- [3] M. Kobusch, Th. Bruns, R. Kumme, Yon-Kyu Park, "Preliminary Investigations of Dynamic Responses of a Multi-Component Force-Moment Sensor Subject to Impulse Forces", *IMEKO TC3*, Celle, Germany, pp. 183-191, 24-26 Sept. 2002.
- [4] A. Täubner, H.-J. v. Martens, "Diffraction grating interferometer for the accurate measurement of rotational quantities", *Measurement*, vol. 16, pp. 71-80, 1995.

---

#### Authors:

Dr. Michael Kobusch, Department 1.1, Physikalisch-Technische Bundesanstalt (PTB), Bundesallee 100, 38116 Braunschweig, Germany, phone +49 531 592 1107, fax +49 531 592 1105, e-mail michael.kobusch@ptb.de;

Dr. Thomas Bruns, Section 1.13, Physikalisch-Technische Bundesanstalt (PTB), Bundesallee 100, 38116 Braunschweig, Germany, phone +49 531 592 1132, fax +49 531 592 1105, e-mail thomas.bruns@ptb.de